

4-2014

Mathematical Analysis of ALS Biochemistry

Emily Rose Bainwol
College of William and Mary

Follow this and additional works at: <https://scholarworks.wm.edu/honorstheses>

 Part of the [Applied Mathematics Commons](#), [Chemicals and Drugs Commons](#), and the [Chemistry Commons](#)

Recommended Citation

Bainwol, Emily Rose, "Mathematical Analysis of ALS Biochemistry" (2014). *Undergraduate Honors Theses*. Paper 12.
<https://scholarworks.wm.edu/honorstheses/12>

This Honors Thesis is brought to you for free and open access by the Theses, Dissertations, & Master Projects at W&M ScholarWorks. It has been accepted for inclusion in Undergraduate Honors Theses by an authorized administrator of W&M ScholarWorks. For more information, please contact scholarworks@wm.edu.

Mathematical Analysis of ALS Biochemistry

by Emily Rose Bainwol

Abstract

The purpose of this research is to further characterize the apoptotic pathways involved in a neuron affected by familial ALS. ALS is an aggressive disease that affects many people presently. However, research on neurodegeneration as it specifically pertains to ALS is limited because research on more common neurodegenerative diseases takes priority. The main objective of this research is to create a greater understanding of some of the major defining features of ALS - including mutated SOD1 gene, excitotoxicity, and organelle dysfunction. The hope is that this will help current research on the disease develop more effective treatments and, eventually, possibly even a cure.

Copper-Zinc Superoxide Dismutase (SOD1) codes for an enzyme critical for breakdown of metabolic waste – specifically reactive oxygen species such as hydrogen peroxide. Mutated forms of SOD1 lead to accumulated waste in the cells. This contributes to the development of other apoptotic factors – including apoptosome formation – within the cell. With this project, the combined effects of this waste accumulation and other outcomes of mutated SOD1 will be investigated. The ultimate goal is to identify how those effects lead to increased risk for ALS onset.

The current clinical literature on ALS has been researched in order to identify and explore a number of mutations at the SOD1 gene that are linked to the disease. The relevant literature is used to create a biochemical model of SOD1 processes and all of the involved chemical species using a freeware program, Cell Designer. The data will be quantitatively

analyzed by creating a mathematical model of the biochemical model. With this mathematical model, it will be easier to identify which ones play important roles in ALS onset and progression.

1. Introduction

Amyotrophic Lateral Sclerosis (ALS) is a neurological disease in which degeneration of motor neurons leads to muscle atrophy. Several factors contribute to ALS onset, making it difficult to determine initial trigger points. These factors include reactive oxygen and nitrogen species, excitotoxicity, organelle dysfunction and mutation of the SOD1 gene. This study uses biochemical systems theory (BST) to analyze a model displaying the major biochemical pathways that occur within a neuron subject to the effects of ALS. The model mainly emphasizes effects of mSOD1 and organelle dysfunction, as well as the pathways affected downstream, on neuronal cell death.

BST was created by Savageau (1969) and modified in our research group by Sass et al. (2009). This program utilizes system equations to create a mathematical framework of a biochemical system (in this case, within a neuron). The mathematical framework helps determine both the individual and overall effects of reactions that take place within the neuron. BST is extremely useful when previously conducted experiments do not provide sufficient information about species concentrations (and their effects within the cell) or when current experimental studies are unable to do so.

In this study, BST was used to evaluate different states of an ALS-affected neuron. First, a baseline ALS state was created in which all reactions were assigned arbitrary, relative numerical values. Certain ALS trigger points within the biochemical pathways were located and their mathematical values increased to mimic the disease state in the neuron. Various treatment states

were created. These created decreased mathematical values of the different combinations of processes that lead to the disease state, such as aggregation of mSOD1 protein. The results of the data from the treatment states in comparison to the data from the disease state could potentially yield useful insight for future experimental studies on ALS.

Please refer to earlier work from our lab using the same approach to model and evaluate neurodegenerative diseases (Sass et al., 2009; Yeager & Coleman, 2010; Broome & Coleman, 2011).

2. Methods

Cell Designer (Funahashi et al., 2003) was used to create a visual model of the biochemical pathways, which were then assigned mathematical parameters and entered into the Power Law Analysis and Simulation (PLAS) program (<http://www.dqb.fc.ul.pt/docentes/aferreira/plas.html>), to allow mathematical analysis (Kitano et al., 2005). This section presents major pathways included in the ALS model.

2.1 Modeled pathways

2.1.1 Aggregation of mutated SOD1 protein

The accumulation of mutated SOD1 protein is the first step shown in the model, and it leads to the alteration of many other cellular pathways both directly and indirectly. All of the pathways involving mSOD1 aggregation eventually result in apoptosis of the neuron. One of these pathways is the exiting of cytochrome c from the mitochondria. This causes the activation of caspase-9, which then catalyzes a series of reactions that eventually result in apoptosis (Slee et al., 1999). Mutated SOD1 contributes to this pathway by catalyzing the activation of CHOP protein in the endoplasmic reticulum (Soo et al., 2012). CHOP then works with Bim protein in

the ER to catalyze the translocation of phosphorylated Bax to the mitochondria, where it forms the MAC channel. This channel catalyzes the transport of cytochrome c out of the mitochondria and into the cytoplasm (Jiang et al., 2011; Laurent et al., 2006; Slee et al., 1999; Soo et al., 2012). Refer to Model 1 for a more comprehensive view of this process. This is one of several outcomes discussed in this paper for the involvement of mSOD1 in neuronal apoptosis.

2.1.2 Formation of reactive oxygen and nitrogen species

Reactive oxygen and nitrogen species that are produced in a neuron affected by ALS are a major cause of apoptosis. The formation of hydroxyl radical from hydrogen peroxide, catalyzed by iron in the lysosome, results in the activation of protein kinase A (PKA) (Jiang et al., 2011; Li et al., 2011; Shkolnik et al., 2011). PKA activates NF Kappa-Beta, a eukaryotic transcription factor for the Fas ligand (see Model 2 and section 2.1.9) (Bilak et al., 2004; Beckers et al., 1989, Kasibhatla et al., 1998, Parry et al., 1997; Wajant, 2002). Activation of this protein is also catalyzed by the formation of superoxide anion and peroxynitrite (Shkolnik et al., 2011). Activation of NADPH Oxidase in the lysosome leads to superoxide anion formation (also in the lysosome) (Boillée et al., 2008; Harraz et al., 2008). This then results in the accumulation of peroxynitrite in the neuron (Szabó, 1996).

2.1.3 Caspase activation

The activation of caspases 1,2,3,8, and 9 all trigger the activation of multiple cell processes that result in neuronal apoptosis. Caspase-1 catalyzes the activation of interleukin 1-beta (Birell et al., 2011; Meissner et al., 2010). This in turn activates COX-2 gene transcription (Cheng et al., 2000; Consilvio et al., 2004). COX-2 protein then catalyzes the first step in the arachidonic acid cascade, in which arachidonic acid is converted to the prostaglandin

endoperoxide PGG₂. The result of this cascade is Ca²⁺ influx (Li et al., 2011; Sureda, 2000), which accumulates in the cell, leading to apoptosis (see 2.1.4). A similar cascade of events results in the activation of caspase-9, which is cleaved from its inactive form by the apoptosome that forms as a result of cytochrome c exiting the mitochondria. See Model 3 for a more complete representation of this caspase cascade.

2.1.4 Ca²⁺ accumulation

Ca²⁺ accumulation in the endoplasmic reticulum, mitochondria, and cytosol is a major contributor to neuronal apoptosis. The buildup of Ca²⁺ catalyzes many reactions, including those that result in the dysfunction of the ER and mitochondria. Reactions of importance to this study that are catalyzed by Ca²⁺ and occur in the cytosol include activation of nitric oxide synthase and of phospholipase A2 (Jiang et al., 2011; Liñares et al., 2006). NO synthase activation creates a buildup of nitric oxide, leading to peroxynitrite buildup, which is toxic to the cell (Szabó, 1996; Liñares et al., 2006). Phospholipase A2 (activated by cytosolic Ca²⁺) catalyzes the arachidonic cascade (Jiang et al., 2011). Products of this cascade trigger reactions downstream resulting in apoptosis. All of the reactions catalyzed by intracellular Ca²⁺ in this study (e.g. Fas signaling and ER dysfunction) eventually lead to apoptosis (see Model 2).

2.1.5 Golgi dysfunction

Golgi dysfunction initiates with the translocation of caspase-2 to the Golgi apparatus, where it catalyzes cleavage of Golgin 160 (Jiang et al., 2011). Golgins play a role in membrane structure and stability, which are at risk when golgins lose their function via cleavage (Barr & Short, 2003). When cleaved, Golgin 160 is a main contributing factor to Golgi dysfunction. Caspase-3, caspase-7, and ER stress also contribute to Golgin 160 cleavage (Hicks & Machamer,

2005). Another trigger point for Golgi dysfunction is the buildup of mixed lineage kinase-3 (MLK3) in the cytoplasm (Cha et al., 2004). MLK3 is responsible for phosphorylation of Golgin 160, which leads to excess cleavage.

Additionally, cleavage of other proteins within the Golgi inhibits their normal function and also leads to Golgi dysfunction. One such protein is the transport factor p115, which is involved in ER-Golgi traffic (Barr, 1999). When normally functioning, P115 forms a complex with GRASP65, GM140, and Giantin (Hicks & Machamer, 2005). This complex aids in correct targeting of proteins to the Golgi. When p115 is cleaved, it is not available for complex formation and Golgi dysfunction results from disrupted protein transport (see Model 4).

2.1.6 Endoplasmic reticulum dysfunction

ER dysfunction in ALS is closely tied to mSOD1 aggregation. Toxic mSOD1 builds up in the cytoplasm and reaches the ER lumen (Soo et al., 2012). This, together with Bim inside the ER, leads to ER stress (Soo et al., 2012). Stress to the ER is directly linked to ER dysfunction. Additionally, mSOD1 in the ER activates CHOP. Active CHOP enhances Bax translocation to the mitochondria, eventually leading to apoptosome formation (Gotoh et al., 2004; Kim et al., 2006) (see Model 1).

Null Hong Kong mutant protein (NHK) inside the ER promotes ER stress and therefore ER Dysfunction (Nishitoh et al., 2008). Ubiquitination of NHK prevents this. When mSOD1 is present, it joins with Derlin1 to form a complex. This complex inhibits ubiquitination of NHK. In this way, mSOD1 inhibits inhibition of ER stress (see Model 5).

2.1.7 Mitochondrial dysfunction

Mitochondrial dysfunction is closely tied to ER dysfunction via CHOP and calcium buildup. Dysfunction within the mitochondria results mainly from calcium buildup and caspase activation. Calcium translocates from the ER to the mitochondria, where it contributes to mitochondrial dysfunction (Kuwana et al., 2003). Caspase-3 and caspase-8 both contribute to mitochondrial dysfunction as well (Li et al., 1998) (see Model 6). Mutated SOD1 plays a role as well, as it enhances translocation of cytochrome c out of the mitochondria and into the cytoplasm (Takeuchi et al., 2002), as shown in Model 6. In the cytoplasm, cytochrome c forms the apoptosome with Apoptotic protease activating factor 1 (APAF 1) and activates the caspase cascade. Caspase-3 and caspase-8 are then available to further inhibit normal mitochondrial function.

2.1.8 Glutamate excitotoxicity

Calcium buildup contributes largely to glutamate excitotoxicity. Calcium buildup in the astrocyte aids in activation of the arachidonic acid cascade, eventually leading to PGE2 formation in the astrocyte (Consilvio et al., 2004; Jiang et al., 2011). PGE2 then promotes glutamate exiting the astrocyte into the synapse. The postsynaptic neuron picks up the excess glutamate. Once in the neuron, glutamate activates NF-KappaB, which initiates Fas signaling via FasL transcription (Wajant, 2002) (see 2.1.9 and Model 2). Glutamate toxicity also promotes toxic mSOD1 buildup and formation of reactive nitrogen species (Harraz et al., 2008; Szabó, 1996). The peroxynitrite that results also contributes to FasL transcription by activating PKA (see 2.1.2 and Model 2). Refer to Model 7 for a schematic overview of the effects of glutamate toxicity.

2.1.9 Fas signaling

Fas ligand binds to its receptor and forms a complex. This complex promotes accumulation of reactive oxygen species, thus contributing to apoptosis (Cheng et al., 2010; Vercammen et al., 1998). Fas and Fas ligand then form the death-inducing signaling complex (DISC), where they are joined with Fas-Associated protein with Death Domain (FADD) (Wajant, 2002). FADD is an adaptor molecule that bridges Fas-receptor and other death receptors to caspase-8, which is also a component of DISC (see Model 2). DISC promotes activation of caspase-8, which leads to mitochondrial dysfunction and p115 cleavage (see 2.1.5 and 2.1.7). Therefore DISC plays a large role in organelle dysfunction.

2.2 PLAS

The Power Law Analysis and Stimulation (PLAS) program uses mathematical equations to predict changes in concentrations of species of interest over time. Each pathway in the model was assigned a numerical value. Each of the n species involved was assigned a variable ($X_1 - X_n$).

2.2.1. Initial variables

Each chemical species (e.g. protein, enzyme, ion) was assigned an X-value. Species that were not affected by any other species (regardless of whether or not they had an effect on other species) were labeled as independent, whereas those that were affected by at least one other species were labeled as dependent. Initial concentrations were given to each X-value. These concentrations were based on the species' assumed *relative* concentrations, which were estimated from the data provided by the literature. More details regarding PLAS can be found in previous reports from our lab (Sass et al., 2009).

2.2.2. System equations

Each X-value was used to create a system equation. Numerical J-values were assigned to each reaction in the biochemical model in order to identify them. J-values were then added to or subtracted from each system equation. J values leading to the formation of species X are positive and those leading away from X are negative. For example, amyloid-beta protein is formed from degraded amyloid-beta protein precursor (APP) (J2) and amyloid-beta aggregate is accumulated from amyloid-beta (J3). Thus the system equation for amyloid-beta (X4) is $X4' = J2 - J3$.

2.2.3. Flux Equations

A rate constant, k, was assigned to each process in the baseline state. The k values vary based on the rates of reactivity for each reaction. For example, accumulation of mSOD1 in the mitochondria (J81) is due to the presence of toxic cytoplasmic mSOD1 (X8). The flux equation for mitochondrial mSOD1 accumulation is $J81 = k81 X8^{g818}$, with k81 and g818 as rate-determining constants. These constants are generally left as 1.00. Species that act as catalysts for the reactions (promote formation of X) are positive and given a rate constant p (promoting). Those that inhibit the reactions are negative and given a rate constant i (inhibiting). P-values are usually left as 1.00 and i-values are usually left as -1.00. For example, formation of caspase-9 (J26) from procaspase-9 (X32) is catalyzed by the Apaf 1 – cytochrome c complex (X28) (see 3.1.1) and inhibited by XIAP protein (X76). The flux equation for this reaction is $J26 = k26 X32^{g2632}$. The value for k26 in the baseline state is .01, and the rate, which initially remains small for baseline conditions, is given by $k' = .0001*(p2628 X28 + i2676 X76)$.

2.2.4. Excel Spreadsheets

For each X-value, PLAS determines concentrations over a pre-determined time interval. The data output in table form was copied into an Excel spreadsheet in order more easily manipulate a

graphical analysis of the data. This was done for the baseline state, disease state, and treatment state for each X-value chosen. The formula used for the disease state graphs was (disease-baseline)/baseline in order to evaluate the concentration changes as a percentage of certain X-values from baseline state to disease state. Similarly, the formula used for the treatment state graphs was (treatment-disease)/disease to evaluate percent change in concentrations from disease state to treatment state. This allowed for a better visual interpretation of the data by showing the trends certain X-values had in any given state.

3. Results

3.1 Apoptotic levels

3.1.1 Disease model

The rate of apoptosis increases dramatically with the increase of cytosolic Ca^{2+} . Ca^{2+} in the cytosol of the neuron contributes to buildup of stress to the endoplasmic reticulum (Jiang et al., 2011; Soo et al., 2012), which results in mSOD1 aggregation. The increased activation and accumulation of apoptotic factors (including mSOD1) and other cellular abnormalities (such as those described in 3.3 – 3.5) also contributed to the greater rate of apoptosis in the disease model.

Bax translocation from the cytosol to the mitochondria is a large contributor to increased apoptotic levels (Kim et al., 2006). Once in the mitochondria, phosphorylated Bax joins with Bak to form the mitochondrial apoptosis-induced channel (MAC), which catalyzes the release of Cytochrome c into the cytosol. Cytochrome c then joins with Apaf 1 to form the apoptosome, which triggers the caspase cascade via activation of caspase-9 (see Models 1 and 3).

Refer to Figure 1 for comparison of apoptotic levels between disease and treatment states.

3.1.2 Treatment model

The treatment model that resulted in the greatest decline of the major processes contributing to apoptosis (see 3.2-3.5) was created by implementing a cocktail of four pharmaceutical drugs. These drugs have been previously tested and used individually, but not in combination. Minocycline activity was included in the cocktail as an inhibitor of cytochrome c release to the cytosol (Zhu et al., 2002). The decrease in apoptotic levels was enhanced with the administration of this drug alone, confirming its validity as a treatment. Inhibitors of IP₃ activation (XC, 2-ABP, and NSAID) decreased apoptotic levels by indirectly inhibiting Ca²⁺ influx in the cytoplasm (Birrell et al., 2011; Li et al., 2011). While Minocycline was more effective at attenuating apoptotic levels, the cocktail of all four drugs was 1.5 times as effective (see Figure 1).

3.2 Peroxynitrite

3.2.1 Disease model

Peroxynitrite levels in the disease state sufficiently increase due to increased activation of nitric oxide synthase, which is catalyzed by increased cytosolic Ca²⁺ levels (see Model 2). Increased peroxynitrite levels then trigger other pathways that result in apoptosis. One such pathway starts with the activation of PKA (see 2.1.2).

3.2.2 Treatment model

The treatment model was made by inhibiting IP₃ activation. Active IP₃ contributes to Ca²⁺ influx, leading to increased calcium concentration in the cell. Cytosolic calcium causes apoptosis via increased ER stress (see Model 5), activation of NO synthase (see 2.1.4), and activation of Phospholipase A2, which triggers the arachidonic cascade (2.1.4). See Figure 2 for comparison of peroxynitrite concentration for untreated disease state versus treatment state with

IP₃ inhibitors. The effectiveness of existing drugs that inhibit IP₃ (including NSAID, XC, and 2-APB) was mathematically verified in our model. The greatest decrease in apoptotic levels occurred when all three of these inhibitors were simultaneously activated without Minocycline.

3.3 Golgi dysfunction

3.3.1 Disease model

The disease state includes the increased activation of all caspases, and caspase-2 catalyzes the cleavage of Golgin 160 in the Golgi. Inactivation of this protein results in Golgi dysfunction, which leads to apoptosis (Jiang et al., 2011). Cleavage of other proteins, such as GRASP 65 and p115, also result in golgi dysfunction and apoptosis (see Model 4).

3.3.2 Treatment model

IP₃ inhibitors alone proved to be effective in decreasing Golgi dysfunction. Inhibition of IP₃ causes decreased influx of Calcium (see Model 2), which in turn decreases Phospholipase A2 activation. The arachidonic acid cascade is thus inhibited, decreasing levels of PGE2. This inhibits the Fas signaling pathway via inactivation of NF-KappaB (Wajant, 2002). Without Fas signaling, caspase-8 levels are lowered. Since caspase-8 is responsible for p115 cleavage (Chiu, 2002) decreased levels lower Golgi dysfunction.

Minocycline induced the treatment state by inhibiting cytochrome c translocation to the cytosol, therefore inhibiting apoptosome formation and caspase cascade activation (Zhu et al., 2002). Since caspases 2, 3, and 8 are related to Golgi dysfunction via protein cleavage (see 2.1.5), their inactivation contributes to lowered Golgi dysfunction.

According to our model, while IP₃ inhibitors were more effective than Minocycline at decreasing Golgi dysfunction, the cocktail of all four drugs was the most effective treatment. Refer to Figure 3 for a comparison of Golgi dysfunction levels between the disease state and the different treatment states.

3.4 Endoplasmic reticulum dysfunction

3.4.1 Disease model

In the disease state ER dysfunction is caused mainly by ER stress. Many factors contribute to increased ER stress, including cytosolic calcium buildup (increased with IP₃ activation – see Model 2) and toxic mSOD1 within the ER. Mutated SOD1 translocates to the ER lumen in greater concentrations with excess glutamate present (see 3.6.1 and Model 7) (Soo et al., 2012).

3.4.2 Treatment model

IP₃ inhibitors decreased ER dysfunction while Minocycline alone had no effect. Inhibitors of IP₃ decrease calcium influx, which decrease caspase-8 activation (see 3.3.2). Caspase-8 activates caspase-3 (Slee et al., 1999); therefore its inactivation leads to decreased levels of caspase-3. Caspase-3 inactivates EEAT2 receptor and thus increases intracellular glutamate (Boston-Howes et al., 2006) (see Model 7), resulting in excitotoxicity that leads to toxic mSOD1 accumulation in the ER. When caspase-3 is inactivated, this pathway is blocked.

Minocycline prevents caspase cascade activation (Model 3) and therefore decreases caspase-3 activation, leading to decreased glutamate excitotoxicity. While Minocycline alone showed no effect mathematically on ER dysfunction when used as a treatment, the cocktail of all

four drugs (Minocycline and the three IP₃ inhibitors) showed a slightly greater decreasing effect than IP₃ inhibitors alone (see Figure 4).

3.5 Mitochondrial dysfunction

3.5.1 Disease model

Mitochondrial dysfunction in the disease state is increased by the presence of active caspase-8 and caspase-3. The formation of the apoptosome activates the caspase cascade and contributes to mitochondrial dysfunction via caspase-8 and caspase-3 activation. Additionally, caspase-8 activation is increased through Fas signaling (see 2.1.9).

3.5.2 Treatment model

The treatment model that most greatly decreased mitochondrial dysfunction was created by implementing Minocycline alone. Minocycline attenuates the effects of the caspase cascade (including mitochondrial dysfunction) by inhibiting cytochrome c release (see Model 3). IP₃ inhibitors seemed to have no effect on levels of mitochondrial dysfunction. Refer to Figure 5 for a representation of the different treatment states as they apply to mitochondrial dysfunction.

3.6 Glutamate excitotoxicity

3.6.1.1 Disease model

Glutamate excitotoxicity (Model 7) increases with intracellular calcium (see 3.4.2). It promotes mSOD1 aggregation and peroxynitrite levels via increased concentrations of superoxide anion. Intracellular glutamate induces electron transfer from NADPH to molecular oxygen, creating the superoxide anion (Harraz et al., 2008).

3.6.1.2 Treatment model

The treatment state that showed the greatest decrease in glutamate excitotoxicity was created by the implementation of both Minocycline and IP₃ inhibitors (see Figure 6). Minocycline decreases activation of caspases by inhibiting cytochrome c release to the cytosol (see 3.5.2 and Model 3). Decreased caspase 3 activation results in decreased cleavage of EEAT receptor, allowing for intracellular glutamate to exit the neuron (see Model 7). IP₃ inhibitors decrease calcium influx, which decreases NF-KappaB activation and Fas signaling (Wajant, 2002). Absence of Fas signaling results in reduced caspase-3 activation, which is responsible for EEAT cleavage (see 3.4.2). Without EEAT cleavage, buildup of intracellular glutamate diminishes (see Model 7). IP₃ inhibitors alone showed no effect on glutamate excitotoxicity. However, the cocktail of both IP₃ inhibitors and Minocycline showed a greater mathematical decrease in glutamate toxicity than Minocycline alone.

4. Discussion

4.1 Disease Model

Glutamate toxicity increases with calcium influx and caspase activation, resulting in toxic mSOD1 buildup in the ER lumen which then enters the ER. The ER stress that results from the increase of cytosolic calcium concentration then leads to aggregation of mSOD1 in the ER. Mutated SOD1 then activates CHOP protein in the ER, which, together with Bim, catalyzes the translocation of phosphorylated Bax to the mitochondria.

Mitochondrial Bax then gives rise to MAC Channel formation, catalyzing the exiting of cytochrome c from the mitochondria into the cytosol. The translocation of phosphorylated Bax to the mitochondria also contributes to cytochrome c exiting the mitochondria by forming the MAC channel. In the cytosol, cytochrome c joins with Apaf 1 to form the apoptosome, which then

triggers the caspase cascade (and further promoting glutamate toxicity) via activation of caspase-9. Increased cytosolic calcium concentration contributes to this process by facilitating the buildup of ER stress. The increased ER stress relative to that of the Golgi and mitochondria is worth noting for future studies. It also suggests that treatments focused on directly inhibiting ER stress buildup may be more effective than treatments inhibiting processes that induce stress to other organelles.

Increased cytosolic calcium also causes activation of nitric oxide synthase, which then synthesizes nitric oxide. Nitric oxide then combines with the superoxide anion from the lysosome to create peroxynitrite, which activates PKA. PKA, together with PGE2 (a product of the arachidonic cascade), activates NF-KappaB. This leads to Fas signaling, resulting in caspase activation and apoptosis.

The role the Golgi apparatus plays in apoptosis is especially noteworthy because that role is lacking detailed discussion in the literature on ALS. The Golgi dysfunction occurs as a result of many apoptotic factors, including apoptosome formation. The apoptosome that forms in response to processes set in motion by mSOD1 aggregation triggers the caspase cascade, which leads to cleavage and activation of procaspase-2. Caspase-2 then catalyzes the cleavage and inactivation of Golgi 160, which resides in the Golgi. The activation of caspase-2 is a critical part of this process because it cleaves the Golgin 160 protein at a unique site that cannot be cleaved by other caspases, even those with very similar structure to caspase-2. Cleavage at this site triggers more cleavage by other caspases at other sites (Mancini et al., 2000). When Golgi 160 is inactivated, Golgi dysfunction results and leads to neuronal apoptosis. This occurs with cleavage of other golgi proteins (e.g. p115) as well. Cleavage of such proteins is enhanced by caspases.

4.2 Treatment Model

Of the existing drugs included in this model, Minocycline and IP₃ inhibitors were mathematically verified to be effective in decreasing apoptotic levels. This supports previous findings from research on these drugs.

When a cocktail of both Minocycline and IP₃ inhibitors was implemented, apoptotic levels dramatically decreased. Limiting the cytosolic calcium concentration (via IP₃ inhibitors) in the treatment model dramatically decreased Fas signaling, thus reducing caspase activation and glutamate toxicity. Peroxynitrite levels were also lowered due to reduced activation of NO synthase. The decrease in both glutamate toxicity and calcium influx led to lower levels of ER stress and therefore reduced ER dysfunction.

Inhibition of cytochrome c release by Minocycline lowered caspase activation. Inactivation of caspase-3 and caspase-8 reduced mitochondrial dysfunction. Without activation of caspase-2, Golgi 160 inactivation decreased. Likewise, reduced activation of caspase-3 and caspase-8 led to decreased cleavage of both p115 and GRASP65. As a result, Golgi dysfunction leading to apoptosis was suppressed. Further research on this aspect of the model could be beneficial in potentially finding novel drugs that inhibit pathways involved in ALS onset.

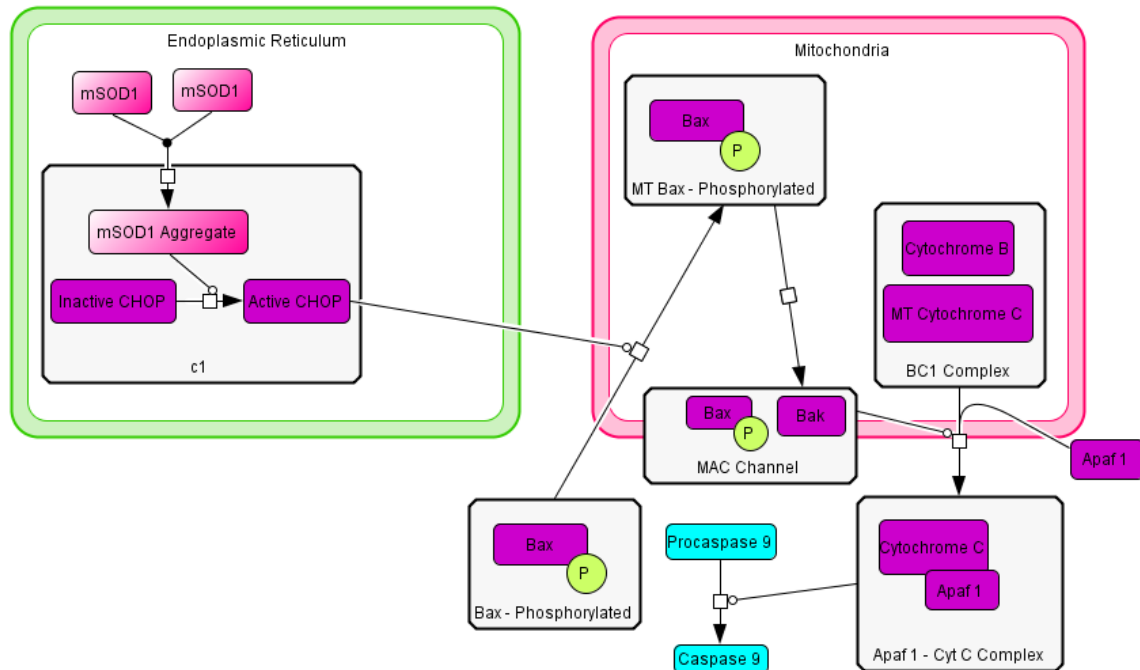
Different aspects of the model – organelle dysfunction, peroxynitrite levels, and glutamate excitotoxicity – varied mathematically in their apparent responses to the different treatment combinations. However, overall apoptotic levels decreased more significantly in the presence of all four drugs in comparison to Minocycline or IP₃ inhibitors alone.

5. Conclusion

The model created and evaluated using BST illustrates various key biochemical processes that contribute to familial ALS onset caused by pathways set forth by SOD1 gene mutation. These key processes include mSOD1 aggregation in the cytosol and the organelles, formation of reactive oxygen and nitrogen species and their toxic effects on the neuron, organelle dysfunction, glutamate excitotoxicity, caspase cascade activation, and Ca^{2+} accumulation in the cytosol of the neuron. In addition to exploring the effects of these and other reactions that occur within a neuron affected by ALS, various existing treatments were tested mathematically to evaluate their ability to decrease levels of apoptosis and apoptotic factors. These treatments were also combined to evaluate their combined effect on apoptotic levels. This ALS model suggests that an effective treatment would be a cocktail of Minocycline and IP_3 inhibitors (XC, 2-ABP, and NSAID). It would be beneficial to research the effect of this cocktail in animal models. This model can theoretically be used to assess the effect of an innovative drug (or cocktail of existing drugs) that acts on any reaction within the model before it undergoes more expensive laboratory tests.

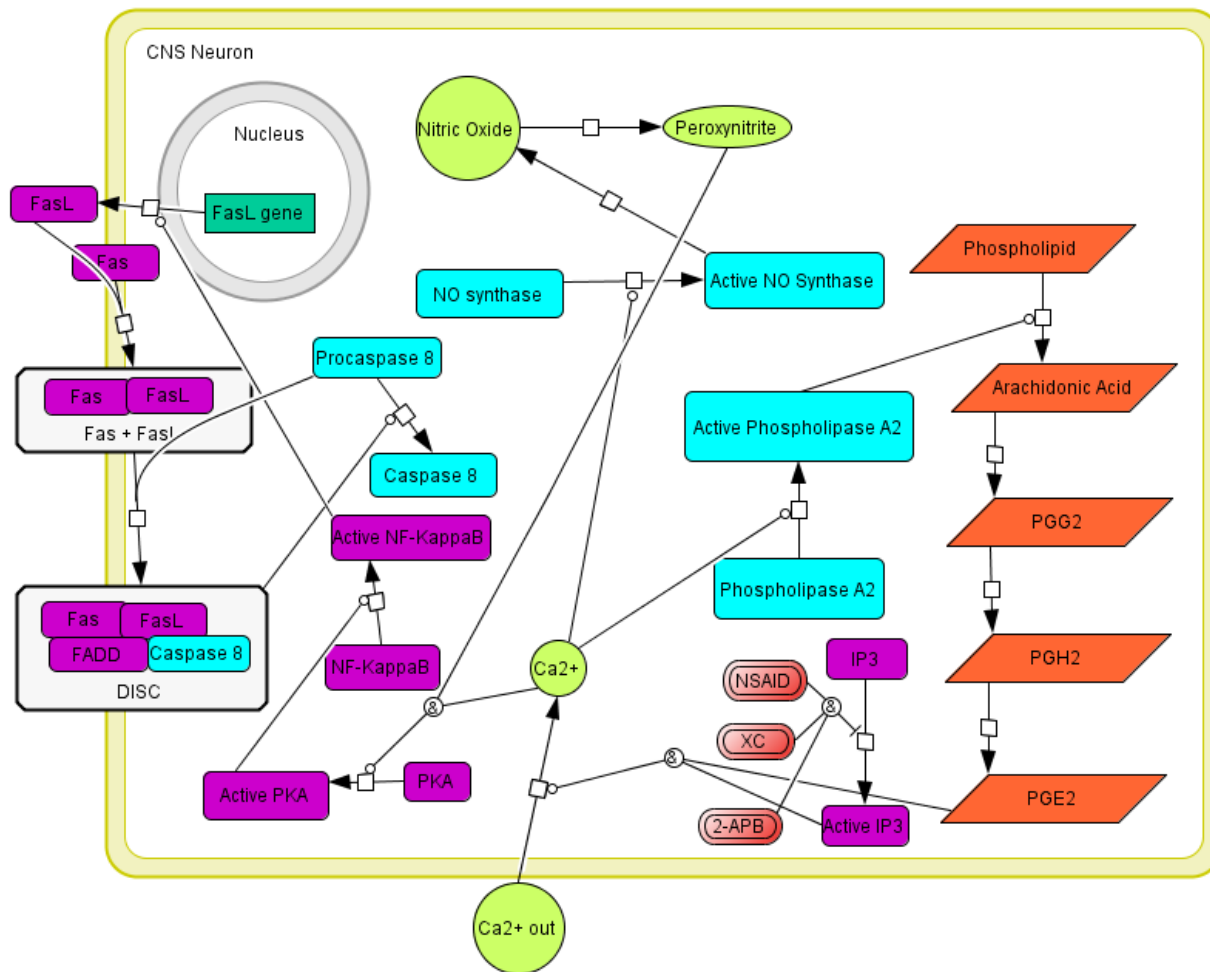
Acknowledgements

This project was funded by William and Mary alumni donors through the Charles Center. The visual model of the biochemical reactions was created using CellDesigner 4.2 (<http://www.celldesigner.org/>). Power Law Analysis and Simulation (PLAS), developed by Antonio E.N. Ferreira (<http://www.dqb.fc.ul.pt/docentes/aferreira/plas.html>), was used to mathematically assess the reactions occurring inside the cell.



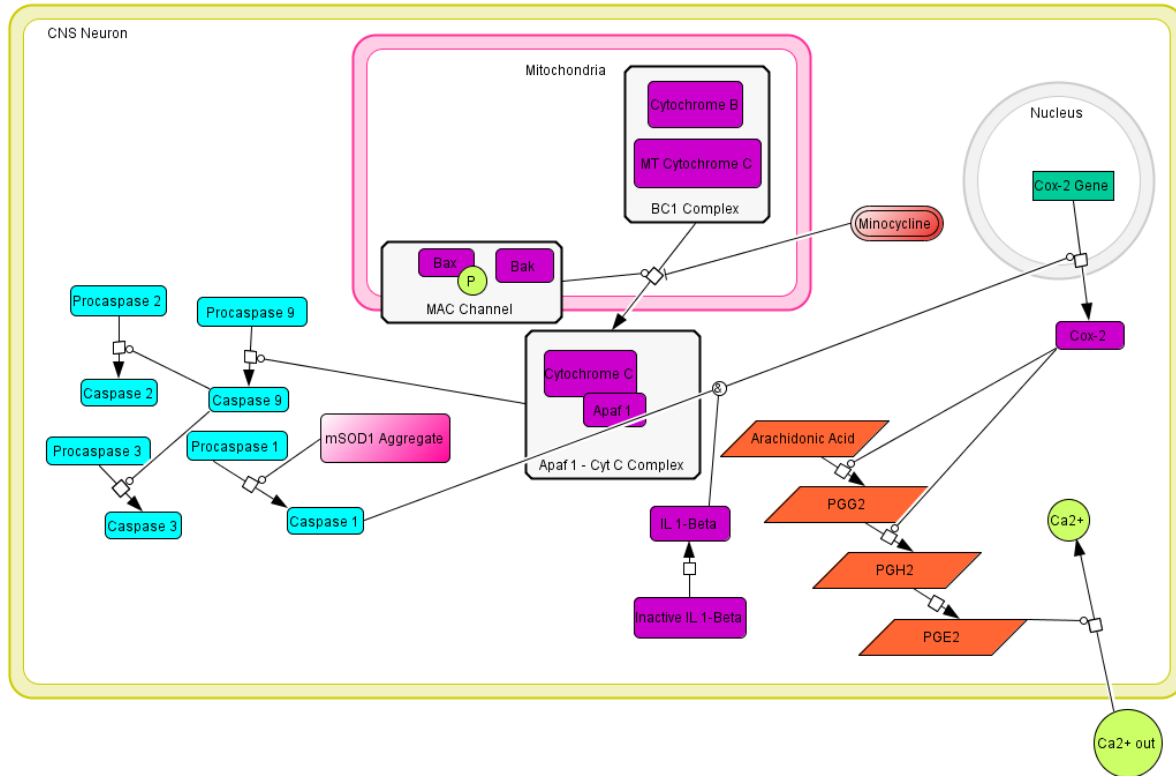
Model 1 Mutated SOD1 aggregation leading to cytochrome c release from mitochondria via CHOP activation

Mutated SOD1 activates CHOP, which catalyzes the translocation of phosphorylated Bax to the mitochondria. This allows for MAC Channel formation, which promotes translocation of cytochrome c from the mitochondria to the cytosol. Once in the cytosol, cytochrome c is free to form the apoptosome complex with Apaf 1, which triggers the caspase cascade via activation of caspase-9.



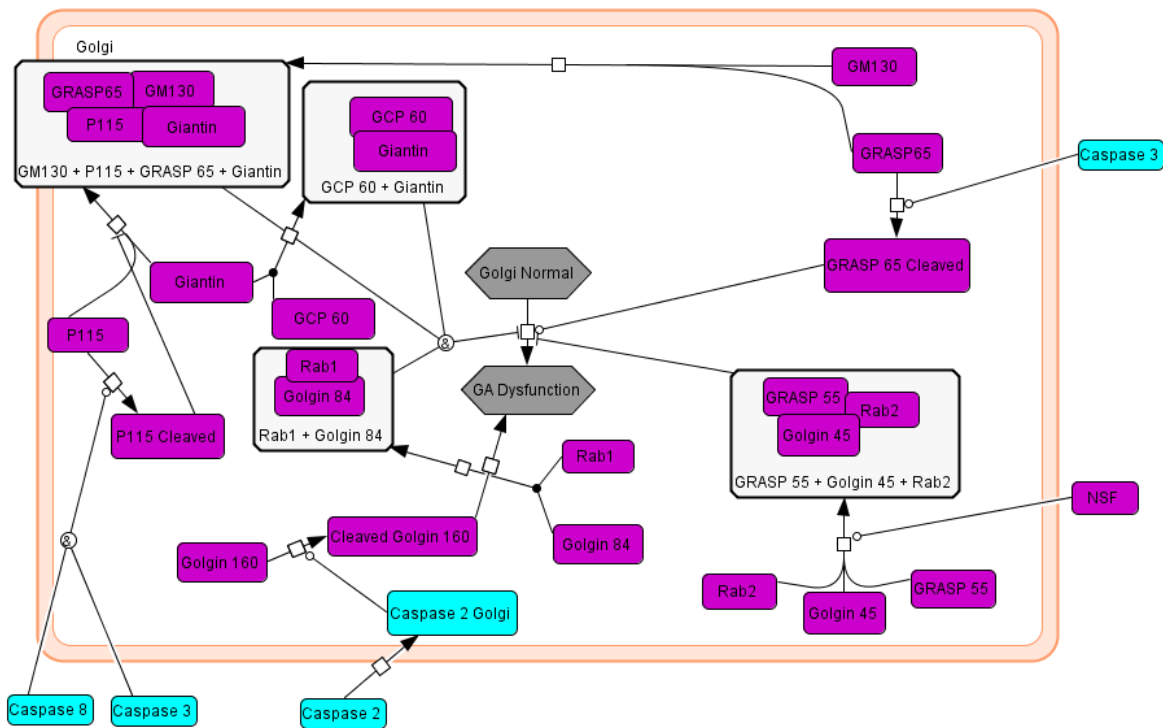
Model 2 Effects of Ca^{2+} and reactive nitrogen species

The accumulation of Ca^{2+} in the cytosol catalyzes both the activation of NO synthase and the start of the arachidonic acid cascade, producing PGE2. PGE2 contributes to further Ca^{2+} accumulation. NO synthase creates nitric oxide, which leads to peroxynitrite synthesis. Both calcium and peroxynitrite contribute to activation of PKA. Active PKA catalyzes the activation of NF-KappaB, which initiates Fas signaling via transcription of Fas ligand. Ca^{2+} influx is enhanced by active IP_3 , which is inhibited by the drugs shown.



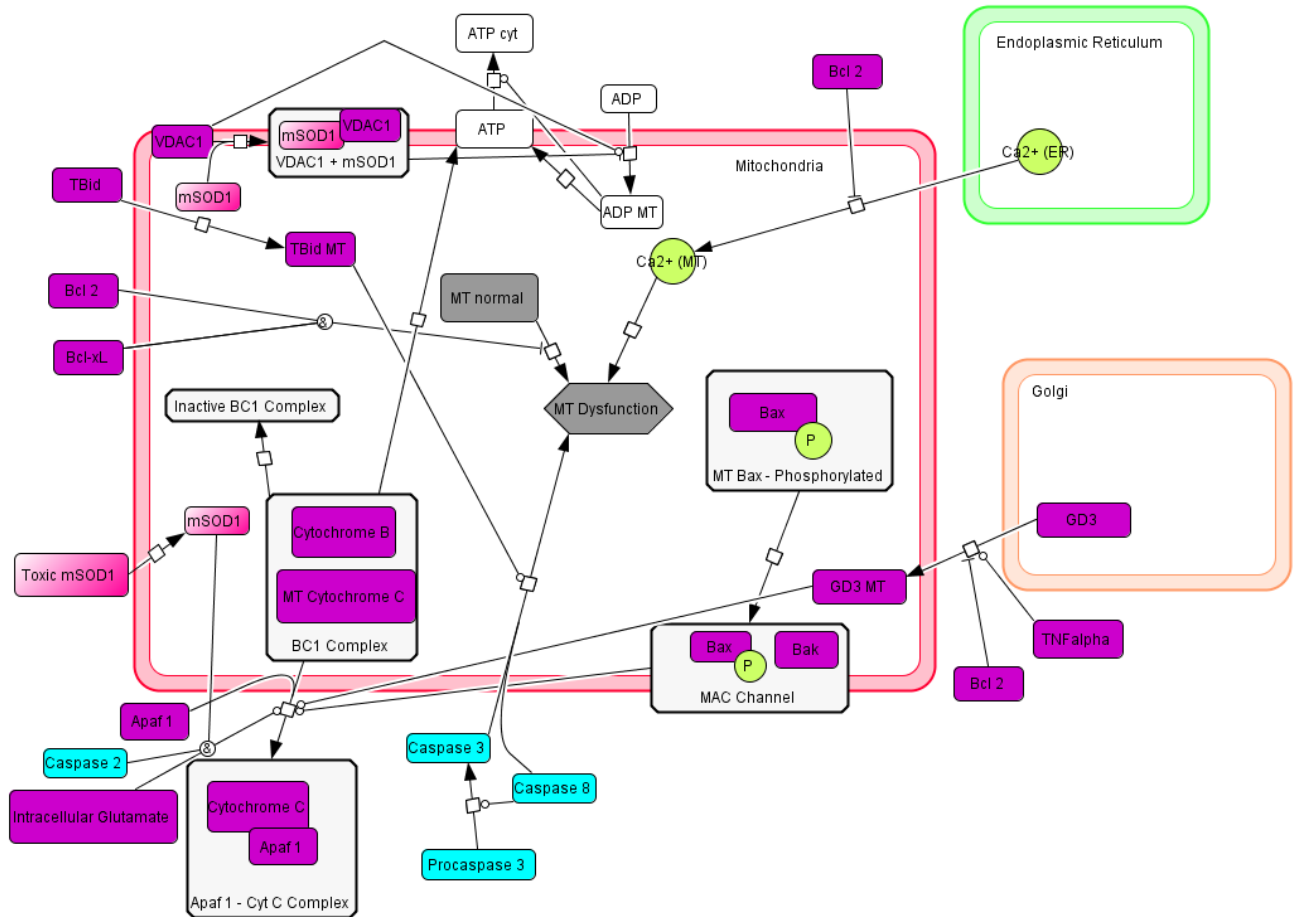
Model 3 Apoptosome formation and caspase activation

Formation of the apoptosome forms when cytochrome c exits the mitochondria into the cytosol. The apoptosome activates caspase 9, which triggers the caspase cascade. One effect of caspase activation is Cox-2 transcription, initiated by caspase 1. This activates the arachidonic acid cascade, resulting in calcium influx.



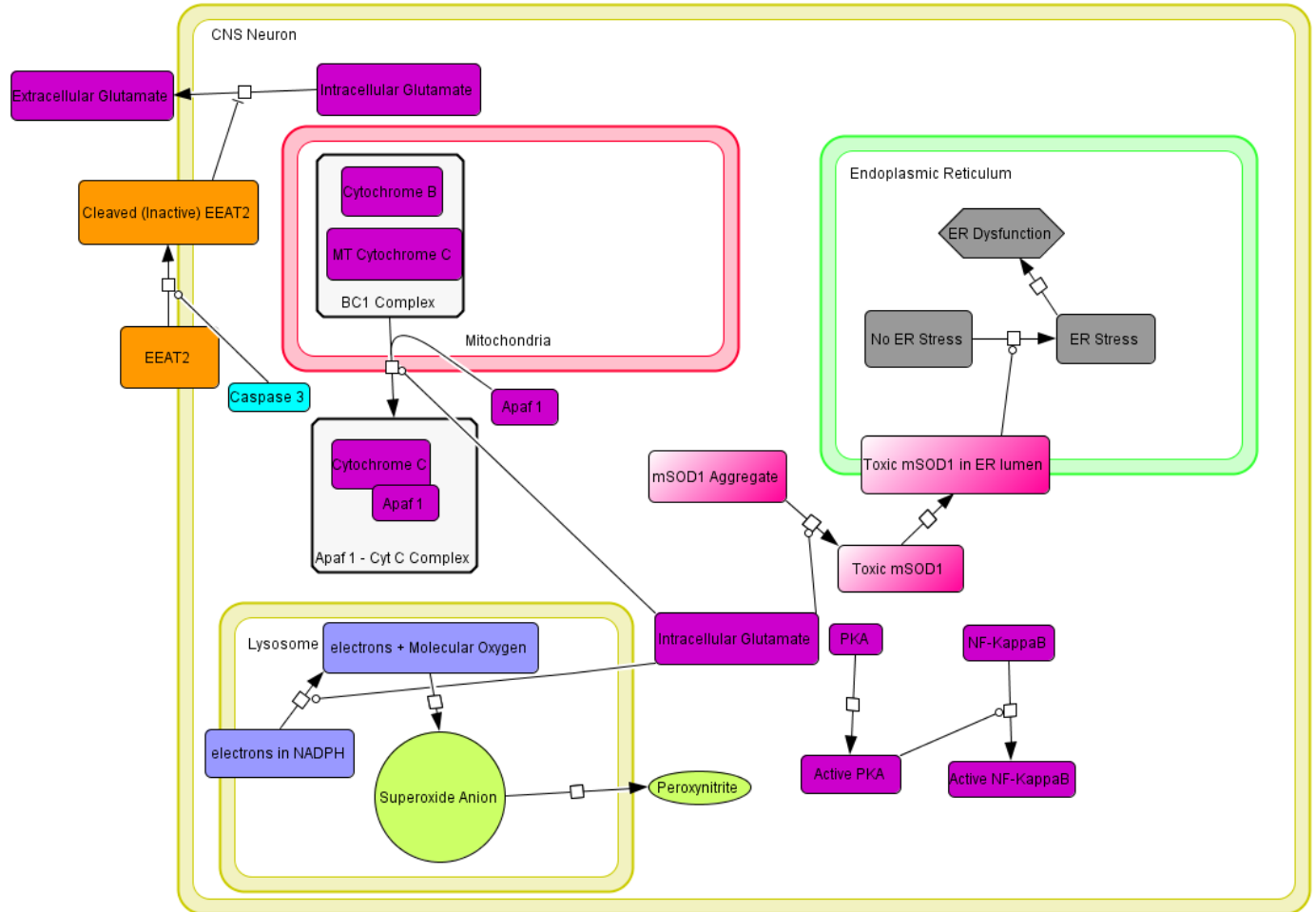
Model 4 Golgi dysfunction

Golgi dysfunction occurs when golgi proteins become cleaved and do not perform their normal function within the golgi. These proteins include Golgin 160 GRASP 65, and p115 – all of which are cleaved by caspases. Complexes formed by normally functioning proteins act to suppress golgi dysfunction. Cleaved products induce dysfunction.



Model 6 Mitochondrial dysfunction

Mitochondrial dysfunction is enhanced with caspase-3 and caspase-8 activation. Mutated SOD1, which promotes cytochrome c release, can be tied back to caspase activation (which increases mitochondrial dysfunction) via activation of CHOP. Additionally, calcium buildup within the mitochondria contributes to organelle dysfunction. Anti-apoptotic factors Bcl 2 and Bcl-xL inhibit dysfunction of the mitochondria.



Model 7 Glutamate excitotoxicity

Intracellular glutamate is increased with inactivation of EEAT2, which is cleaved by caspase-3. Glutamate toxicity leads to increased mSOD1 aggregation, which produces ER stress and dysfunction. Glutamate promotes electron transfer from NADPH to oxygen, creating the superoxide anion. This increases levels of reactive nitrogen species. Cytochrome c release is increased with glutamate toxicity as well.

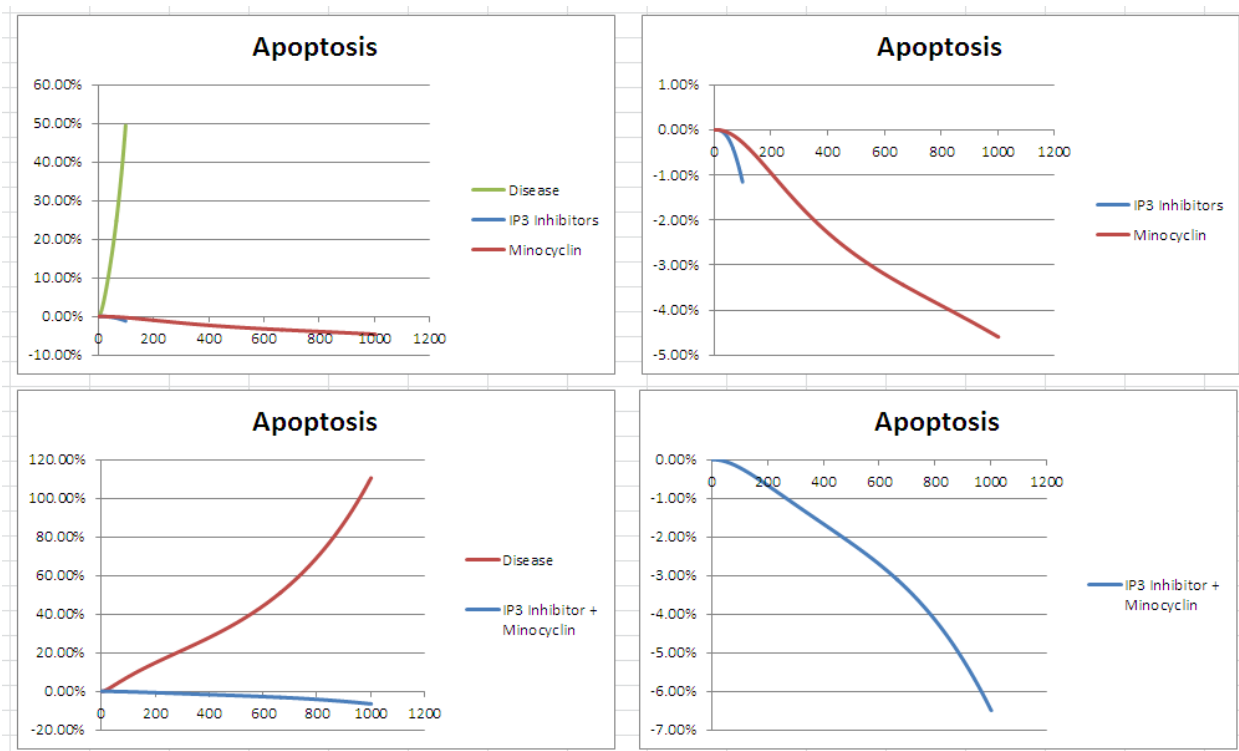


Figure 1: Apoptosis

Apoptotic levels showed the greatest decrease in the treatment state that used both IP₃ inhibitors and Minocycline. The decrease in apoptotic levels was 1.5 times greater than the decrease observed with Minocycline alone.

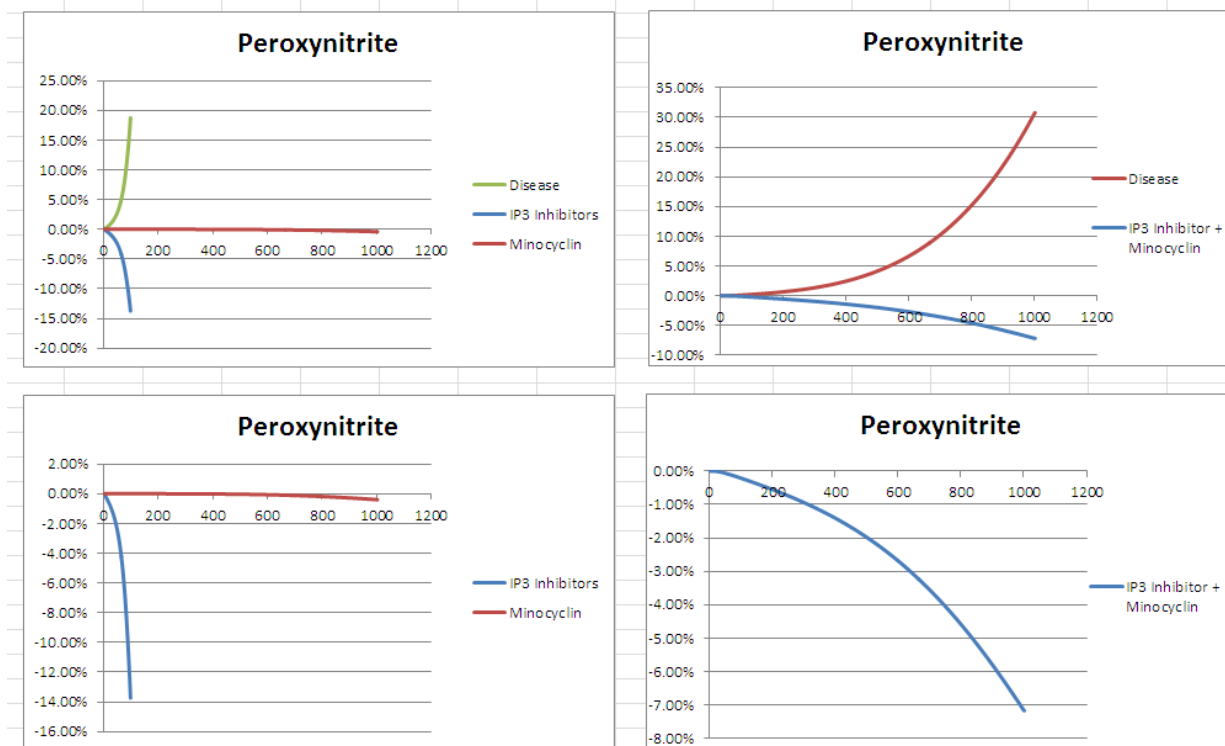


Figure 2: Peroxynitrite

Peroxynitrite levels showed the greatest decrease from disease to treatment state with Mino cyclin alone. The decrease with the cocktail drug was about half of that with Mino cyclin. IP₃ inhibitors showed a very small decrease in comparison to the cocktail drug and Mino cyclin.

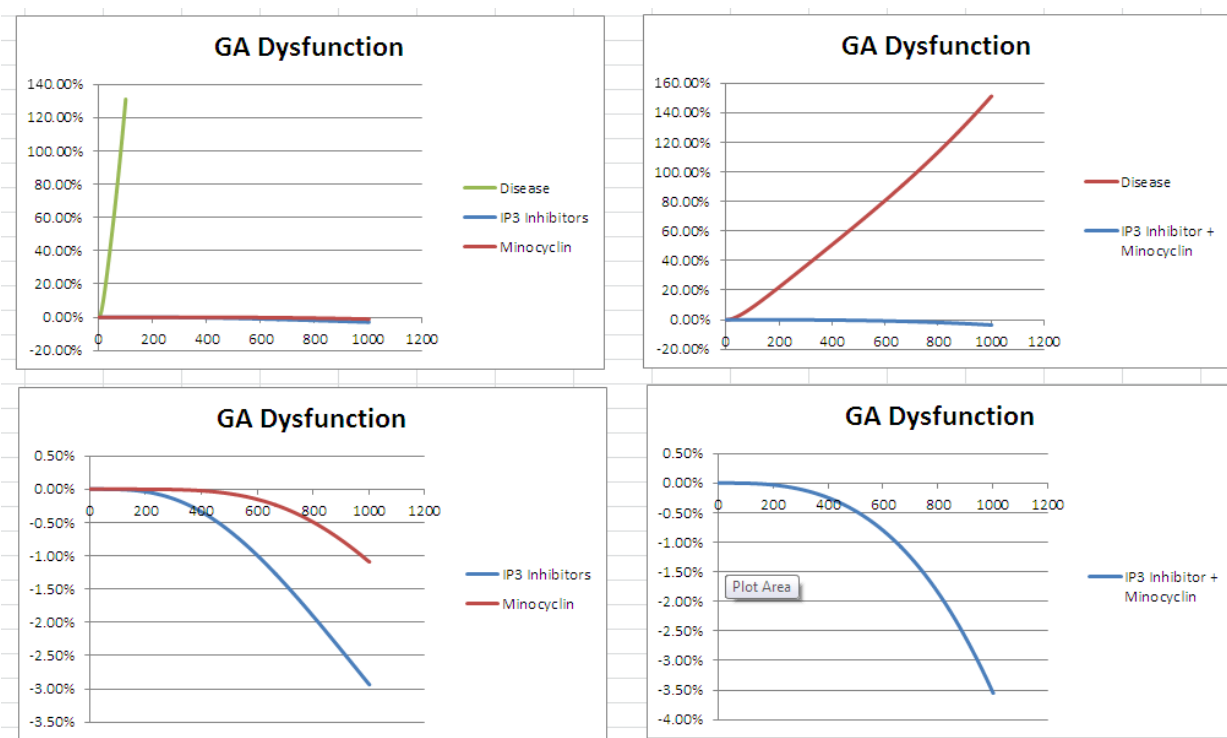


Figure 3: Golgi dysfunction

Golgi dysfunction was decreased with all three treatment states. The most effective treatment state was induced by the use of both IP₃ inhibitors and Minocycline.

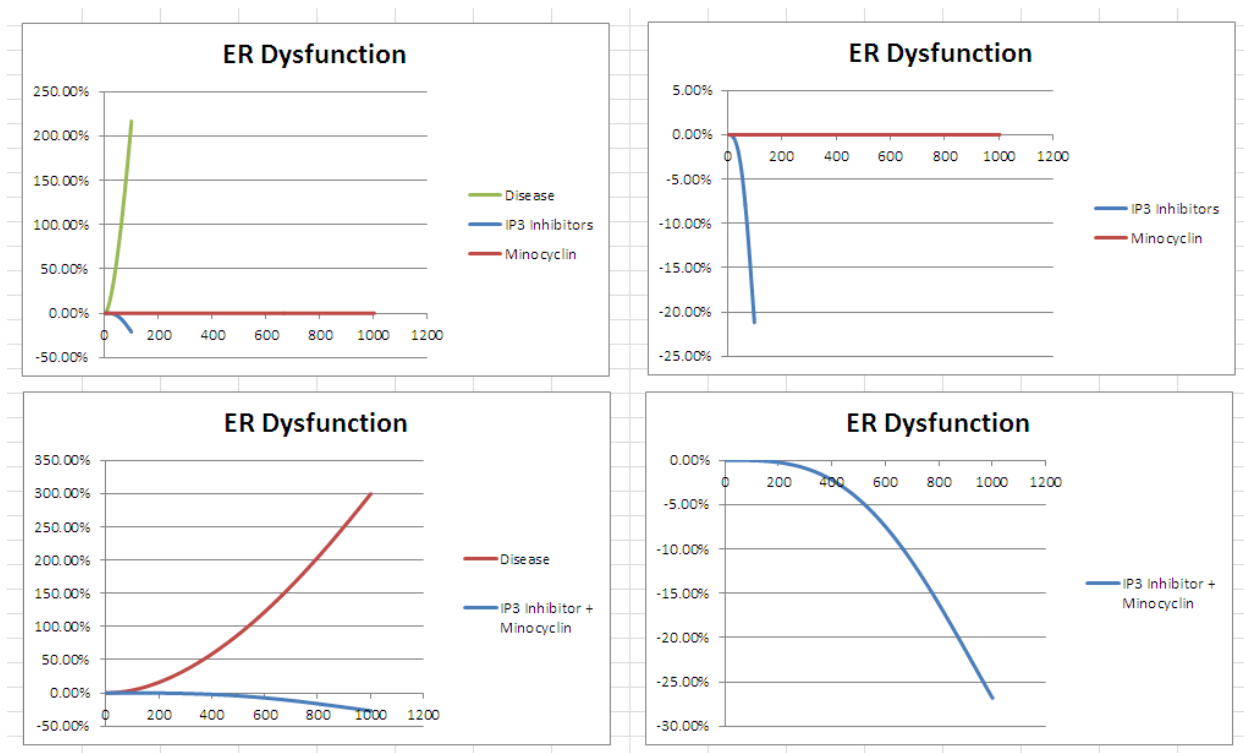


Figure 4: Endoplasmic reticulum dysfunction

ER dysfunction was decreased the most with the use of the both IP₃ inhibitors and Minocycline. IP₃ inhibitors showed no decreasing effect when implemented without Minocycline. While Minocycline alone was effective at decreasing ER dysfunction, the cocktail drug was twenty-five percent more effective.

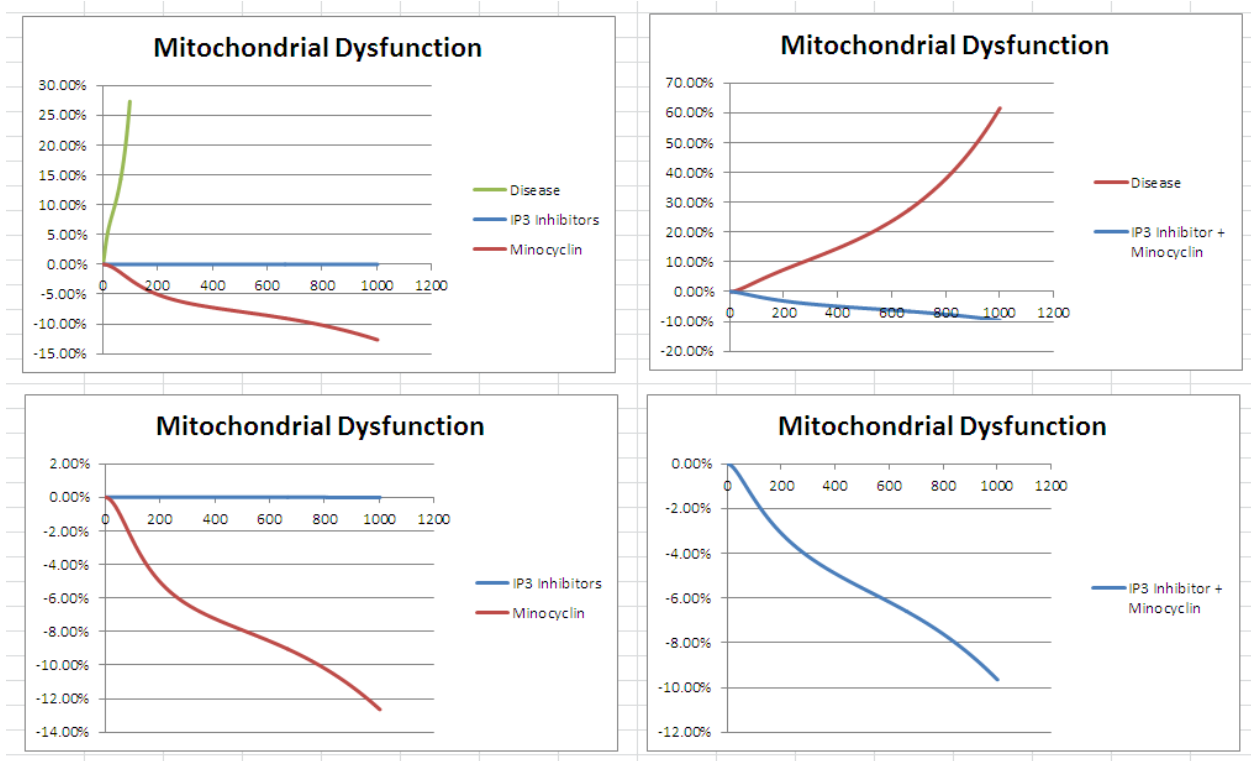


Figure 5: Mitochondrial dysfunction

Minocycline had the greatest decreasing effect on mitochondrial dysfunction in the treatment state. IP₃ inhibitors showed no effect, while the cocktail drug showed a smaller decrease than that of Minocycline.

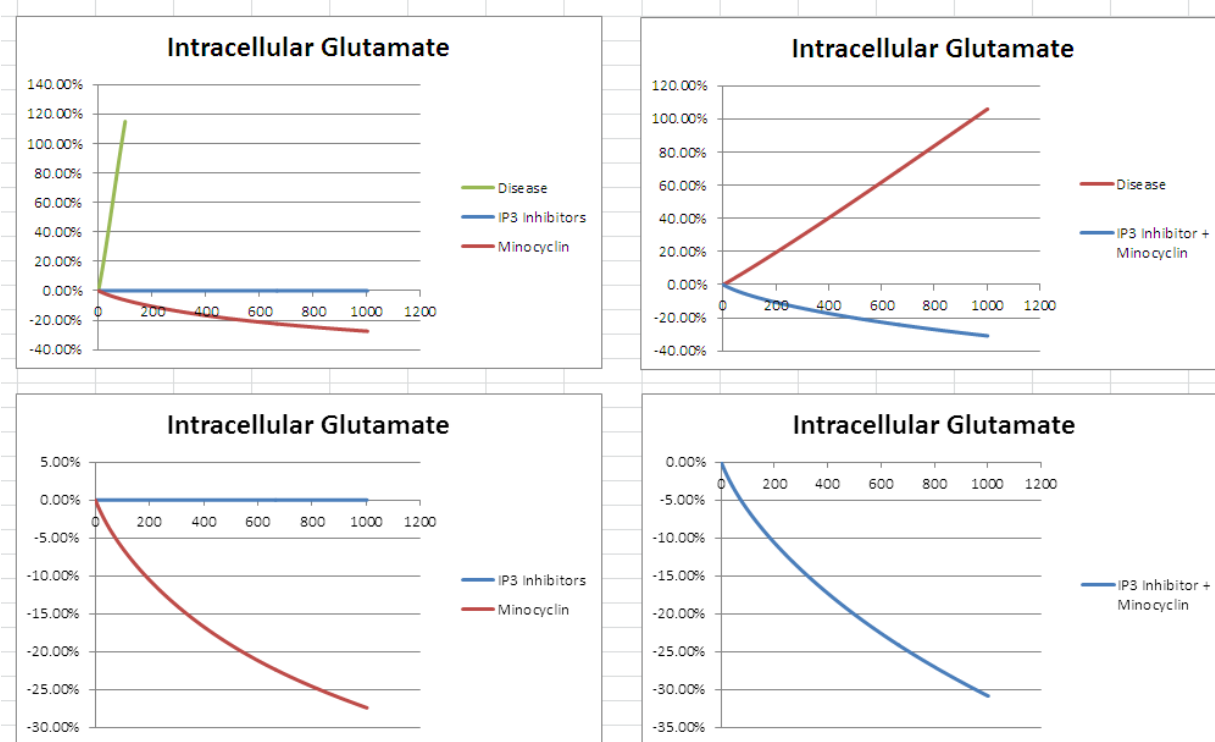


Figure 6: Glutamate excitotoxicity

The use of both IP₃ inhibitors and Minocycline showed the greatest decrease in intracellular glutamate from disease to treatment state. IP₃ inhibitors showed no decreasing effect when used alone. Minocycline decreased intracellular glutamate by more than twenty-five percent, while the cocktail drug decreased it by more than thirty percent.

References

- Barr, F. A. (1999). A novel Rab6-interacting domain defines a family of Golgi-targeted coiled coil proteins. *Current biology*, 9(7), 381.
- Barr, F., Short, B. (2003). Golgins in the structure and dynamics of the Golgi apparatus. *Current opinion in cell biology*, 15(4), 405.
- Beckers, C. J. M., Block, M. R., Glick, B. S., Rothman, J. E., Balch, W. E. (1989). Vesicular transport between the endoplasmic reticulum and the Golgi stack requires the NEM sensitive fusion protein. *Nature (London)*, 339(6223), 397.
- Bilak, M., Wu, L., Wang, Q., Haughey, N., Conant, K., St. Hillaire, C., and Andreasson, K. (2004). PGE2 receptors rescue motor neurons in a model of amyotrophic lateral sclerosis. *Annals of Neurology*, 56(2), 240–248. doi:10.1002/ana.20179
- Birrell, M. A., and Eltom, S. (2011). The role of the NLRP3 Inflammasome in the pathogenesis of airway disease. *Pharmacology & Therapeutics*, 130(3), 364–370. doi:10.1016/j.pharmthera.2011.03.007
- Boillée, S., and Cleveland, D. W. (2008). Revisiting oxidative damage in ALS: microglia, Nox, and mutant SOD1. *The Journal of Clinical Investigation*, 118(2), 474–478. doi:10.1172/JCI34613
- Broome T. M., Coleman R. A. (2011). A mathematical model of cell death in multiple sclerosis. *J Neurosci Methods*, 201(2), 420-425. <http://dx.doi.org/10.1016/j.jneumeth.2011.08.008>
- Cha, H., Smith, B. L., Gallo, K., Machamer, C. E., Shapiro, P. (2004). Phosphorylation of golgin-160 by mixed lineage kinase 3. *Journal of cell science*, 117, 751.

- Cheng, J. P. X., Betin, V. M. S., Weir, H., Shelmani, G. M. A., Moss, D. K. (2010). Caspase cleavage of the Golgi stacking factor GRASP65 is required for Fas/CD95-mediated apoptosis. *Cell death and disease*, 1, e82.
- Cheng, H.-F., Wang, J.-L., Zhang, M.-Z., McKanna, J. A., and Harris, R. C. (2000). Role of p38 in the regulation of renal cortical cyclooxygenase-2 expression by extracellular chloride. *Journal of Clinical Investigation*, 106(5), 681–688. doi:10.1172/JCI10318
- Chiu, R. (2002). A caspase cleavage fragment of p115 induces fragmentation of the Golgi apparatus and apoptosis. *The Journal of cell biology*, 159(4), 637.
- Consilvio, C., Vincent, A. M., and Feldman, E. L. (2004). Neuroinflammation, COX-2, and ALS—a dual role? *Experimental Neurology*, 187(1), 1–10.
doi:10.1016/j.expneurol.2003.12.009
- Funahashi, A., Tanimura, N., Morohashi, M., and Kitano, H., CellDesigner: a process diagram editor for gene-regulatory and biochemical networks, *BIOSILICO*, 1:159-162, 2003
[doi:10.1016/S1478-5382(03)02370-9]
- Harraz, M. M., Marden, J. J., Zhou, W., Zhang, Y., Williams, A., Sharov, V. S., Nelson, K., et al. (2008). SOD1 mutations disrupt redox-sensitive Rac regulation of NADPH oxidase in a familial ALS model. *The Journal of Clinical Investigation*, 118(2), 659–670.
doi:10.1172/JCI34060
- Hicks, S. W., Machamer, C. E. (2005). Golgi structure in stress sensing and apoptosis. *Biochimica et biophysica acta*, 1744(3), 406.
- Jiang, Z., Hu, Z., Zeng, L., Lu, W., Zhang, H., Li, T., and Xiao, H. (2011). The role of the Golgi

- apparatus in oxidative stress: is this organelle less significant than mitochondria? *Free Radical Biology and Medicine*, 50(8), 907–917.
doi:10.1016/j.freeradbiomed.2011.01.011
- Kasibhatla, S., Brunner, T., Genestier, L., Echeverri, F., Mahboubi, A. (1998). DNA damaging agents induce expression of Fas ligand and subsequent apoptosis in T lymphocytes via the activation of NF-kappa B and AP-1. *Molecular cell*, 1(4), 543.
- Kim, B.-J., Ryu, S.-W., and Song, B.-J. (2006). JNK- and p38 Kinase-mediated Phosphorylation of Bax Leads to Its Activation and Mitochondrial Translocation and to Apoptosis of Human Hepatoma HepG2 Cells. *Journal of Biological Chemistry*, 281(30), 21256–21265. doi:10.1074/jbc.M510644200
- Kitano H, Funahashi A, Matsuoka Y, Oda K. Using process diagrams for the graphical representation of biological networks. *Nat Biotechnol* 2005;23(August(8)):961–6.
- Kuwana, T., and Newmeyer, D. D. (2003). Bcl-2-family proteins and the role of mitochondria in apoptosis. *Current Opinion in Cell Biology*, 15(6), 691–699.
doi:10.1016/j.ceb.2003.10.004
- Laurent M. Dejean, Sonia Martinez-Caballero, Stephen Manon, Kathleen W. Kinnally (2006). Regulation of the mitochondrial apoptosis-induced channel, MAC, by BCL-2 family proteins. *Biochim Biophys Acta*, 1762(2), 191–201.
- Li, X., Cudaback, E., Keene, C. D., Breyer, R. M., and Montine, T. J. (2011). Suppressed Microglial E Prostanoid Receptor 1 Signaling Selectively Reduces TNF α and IL-6 Secretion from Toll-like Receptor 3 Activation. *Glia*, 59(4), 569–576.
doi:10.1002/glia.21125

- Liñares, D., Taconis, M., Maña, P., Correcha, M., Fordham, S., Staykova, M., and Willenborg, D. (2006). Neuronal Nitric Oxide Synthase Plays a Key Role in CNS Demyelination. *The Journal of Neuroscience*, 26(49), 12672–12681.
- Mancini, M., Machamer, C. E., Roy, S., Nicholson, D. W., Thornberry, N. A., Casciola-Rosen, L. A., Rosen, A. (2000). Caspase-2 Is Localized at the Golgi Complex and Cleaves Golgin-160 during Apoptosis. *J. Cell Biol.* 149 (3), 603-612.
<http://stke.sciencemag.org/cgi/content/abstract/jcb;149/3/603>
- Meissner, F., Molawi, K., and Zychlinsky, A. (2010). Mutant Superoxide Dismutase 1-Induced IL-1 β Accelerates ALS Pathogenesis. *Proceedings of the National Academy of Sciences*, 107(29), 13046–13050. doi:10.1073/pnas.1002396107
- Nishitoh, H., Kadowaki, H., Nagai, A., Maruyama, T., Yokota, T., Fukutomi, H., Noguchi, T., Matsuzawa, A., Takeda, K., Ichijo, H. (2008). ALS-linked mutant SOD1 induces ER stress- and ASK1-dependent motor neuron death by targeting Derlin-1. *Genes and Development*, 22(11), 1451.
- Parry, G. C., and Mackman, N. (1997). Role of Cyclic AMP Response Element-Binding Protein in Cyclic AMP Inhibition of NF-kappaB-Mediated Transcription. *The Journal of Immunology*, 159(11), 5450–5456.
- Rizzo, M. T., and Carlo-Stella, C. (1996). Arachidonic acid mediates interleukin-1 and tumor necrosis factor-alpha- induced activation of the c-jun amino-terminal kinases in stromal cells. *Blood*, 88(10), 3792–3800.
- Sass, M. B., Lorenz, A. N., Green, R. L., Coleman, R. A. (2009). A pragmatic approach to biochemical systems

- theory applied to an alpha-synuclein-based model of parkinson's disease. *J Neurosci Methods* 2009;178(April 15 (2)):366–77.
- Savageau, M. A. (1969). Biochemical systems analysis. II. The steady-state solutions for an n-pool system using a power-law approximation. *J Theor Biol* 1969;25:370–9.
- Shkolnik, K., Tadmor, A., Ben-Dor, S., Nevo, N., Galiani, D., and Dekel, N. (2011). Reactive oxygen species are indispensable in ovulation. *Proceedings of the National Academy of Sciences - PNAS*, 108(4), 1462.
- Slee, E. A., Harte, M. T., Kluck, R. M., Wolf, B. B., Casiano, C. A., Newmeyer, D. D., Wang, H.-G., et al. (1999). Ordering the Cytochrome C–Initiated Caspase Cascade: Hierarchical Activation of Caspases-2, -3, -6, -7, -8, and -10 in a Caspase-9–Dependent Manner. *The Journal of Cell Biology*, 144(2), 281–292. doi:10.1083/jcb.144.2.281
- Soo, K. Y., Atkin, J. D., Farg, M., Walker, A. K., Horne, M. K., and Nagley, P. (2012). Bim Links ER Stress and Apoptosis in Cells Expressing Mutant SOD1 Associated with Amyotrophic Lateral Sclerosis. *PLoS ONE*, 7(4). doi:10.1371/journal.pone.0035413
- Sureda, F.X. (2000). Excitotoxicity and the NMDA Receptor. *Eurosiva*.
- Szabó, C. (1996). The pathophysiological role of peroxynitrite in shock, inflammation, and ischemia reperfusion injury. *Shock (Augusta, Ga.)*, 6(2), 79.
- Takeuchi, H., Kobayashi, Y., Ishigaki, S., Doyu, M., and Sobue, G. (2002). Mitochondrial Localization of Mutant Superoxide Dismutase 1 Triggers Caspase-Dependent Cell Death in a Cellular Model of Familial Amyotrophic Lateral Sclerosis. *Journal of Biological Chemistry*, 277(52), 50966–50972. doi:10.1074/jbc.M209356200

Vercammen, D., Brouckaert, G., Denecker, G., Van de Craen, M., Declercq, W. (1998). Dual

signaling of the Fas receptor: initiation of both apoptotic and necrotic cell death

pathways. *The Journal of experimental medicine*, 188(5), 919.

Wajant, H. (2002). *The Fas Signaling Pathway: More Than a Paradigm*. Science (New York,

N.Y.), 296(5573), 1635.

Yeager MP, Coleman RA. In silico evidence for glutathione- and iron-related pathogenesis in

Parkinson's disease. *J Neurosci Methods* 2010;188(4/30 (1)):151–64.

Zhao, W., Beers, D. R., Henkel, J. S., Zhang, W., Urushitani, M., Julien, J.-P., and Appel, S. H.

(2010). Extracellular mutant SOD1 induces microglial-mediated motoneuron injury. *Glia*,

58(2), 231–243. doi:10.1002/glia.20919

Zhu, S., Stavrovskaya, I.G., Drozda, M., Kim, B.Y.S., Ona, V., Li, M., Sarang, S., Liu, A.S.,

Hartley, D.M., Wuk, D.C., Gullans, S., Ferrante, R.J., Przedborski, S., Kristal, B.S.,

and Friedlander, R.M. (2002). Minocycline inhibits cytochrome c release and delays

progression of amyotrophic lateral sclerosis in mice. *Letters to Nature*, 74-75